Vibrational Spectroscopy 92 (2017) 200–214

Contents lists available at ScienceDirect

Vibrational Spectroscopy

journal homepage: www.elsevier.com/locate/vibspec

IR study on the electrochemical generation of a nitro radical anion by a hepatotoxic *N,N′*-disubstituted benzimidazole-2-thione

D. Yancheva[a,*], S. Stoyanov[a], N. Anastassova[a], A.Ts. Mavrova[b]

[a] Institute of Organic Chemistry with Centre of Phytochemistry, Bulgarian Academy of Sciences, Acad. G. Bonchev Str., build. 9, 1113 Sofia, Bulgaria
[b] University of Chemical Technology and Metallurgy, 8 Kliment Ohridski Blvd., 1756 Sofia, Bulgaria

ARTICLE INFO

Article history:
Received 11 February 2017
Received in revised form 7 June 2017
Accepted 8 June 2017
Available online 11 July 2017

Keywords:
Nitroaromatic drugs
1,3-disubstituted-1H-benzo[d]imidazole-2(3H)-thiones
Radical anion
IR
DFT
Electron affinity

ABSTRACT

In the course of our study on the hepatotoxicity of 1,3-disubstituted-1H-benzo[d]imidazole-2(3H)-thiones, we generated and characterized the radical anion of methyl 3-[3-(3-methoxy-3-oxopropyl)-5-nitro-2-thioxo-2,3-dihydro-1H-benzimidazol-1-yl]propanoate which shows the highest toxicity within the studied series. The reduction of the title compound was carried out electrochemically and the spectral and structural changes arising from the conversion were described based on IR spectra and DFT calculations. Repeated monitoring of IR spectra over time demonstrated successful generation of the radical anion accompanied by strong frequency decrease of N—O stretching vibrations and increase of C—N stretching vibration. The neutral compounds and the radical anion are characterized by coplanar orientation of the nitro group towards the aromatic system which most likely contributes to the observed toxicity. The structure of the radical anion shows extended electronic conjugation compared to the neutral compound. The NBO spin population analysis of the radical anion indicated that 0.707 of the odd electron is localized over the nitro group, while 0.293 is spread over the benzimidazole-2-thione fragment. Based on calculated energy of the lowest unoccupied molecular orbital (E_{LUMO}) for the neutral compound, energy difference between the lowest unoccupied and the highest occupied molecular orbital (ΔE_{L-H}), and adiabatic electron affinity (EA), it was estimated that the propensity of methyl 3-[3-(3-methoxy-3-oxopropyl)-5-nitro-2-thioxo-2,3-dihydro-1H-benzimidazol-1-yl]propanoate to generate a radical anion in biological systems would be comparable to that of nitrobenzene and nimesulide and much lower than those of nitrofurantoin.

1. Introduction

Drugs containing a nitroaromatic moiety such as nimesulide, nilutamide, flutamide etc. (Scheme 1) have been associated with hepatotoxicity due to bioreduction of the nitro group and formation of hazardous metabolites [1–5]. The bioreduction of the nitroaromatic compounds undergoes a multistep conversion to nitro radical anions, nitroso intermediates, N-hydroxy derivatives and finally to the respective amines. The process is catalyzed by specific enzymatic systems including primarily cytochrome P450 (CYP) reductase as well as xanthine oxidase, aldehyde oxidase and quinone reductase [5].

The cytotoxicity of these compounds could be due to the emerging reactive intermediates in the process of bioreduction, such as nitroanion radicals, which are capable of binding covalently to nucleophilic centres of proteins and nucleic acids. As a result of the redox cycling the oxidative stress increases, which also contributes to the overall toxicity. Hepatocytes, which were exposed to nitroaromatic drugs like flutamide, demonstrated decrease in the GSH/GSSG ratio [6] and also nitrofurantoin definitely caused intracellular oxidative stress [7].

Therefore, in the study of new drug candidates it is important to characterize the potential reductive products of nitroaromatic compounds. The first step in the mechanism of action of nitroheterocyclic drugs as cytotoxic agents for hypoxic cells is the reduction of the nitro group of the drug to the corresponding nitro radical anion [5].

A series of novel N,N'-disubstituted benzimidazole-2-thione derivatives have been recently synthesized and tested on isolated hepatocytes for their toxicity and antioxidant activity [6]. The effect of the compounds on the functional-metabolic status of the hepatocytes was assessed by monitoring the cell viability and changes in lactate dehydrogenase (LDH), glutathione (GSH) and

* Corresponding author.
E-mail addresses: deni@orgchm.bas.bg (D. Yancheva), s_stoyanov@orgchm.bas.bg (S. Stoyanov), neda.anastassova@gmail.com (N. Anastassova), anmav@abv.bg (A.T. Mavrova).

http://dx.doi.org/10.1016/j.vibspec.2017.06.003
0924-2031/

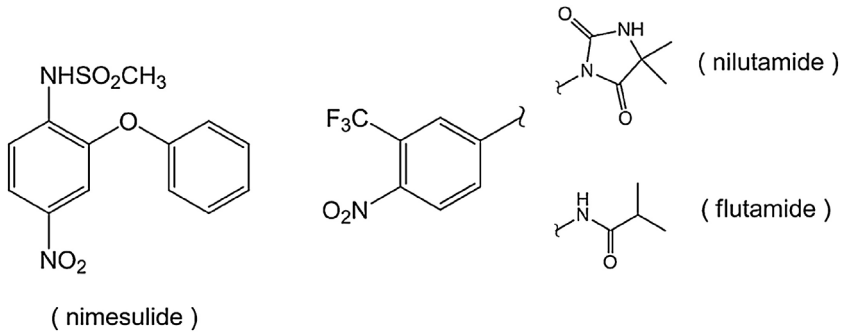

Scheme 1. Chemical structure of nitroaromatic drugs.

malondialdehyde (MDA) levels. The ester substituted in the 5 position of the benzimidazole ring, namely methyl 3-[3-(3-methoxy-3-oxopropyl)-5-nitro-2-thioxo-2,3-dihydro-1H-benzimidazol-1-yl]propanoate (**1,** Scheme 1), showed one of the highest hepatotoxicity compared to the other derivatives bearing a methyl and a benzoyl group as well as one unsubstituted compound [8]. The studies revealed that the least toxic compound containing a benzoyl group led to a drop of the cell viability only by 27%, while **1** demonstrated much higher toxicity and induced a statistically significant decrease by 47% compared to the non-treated hepatocytes. The reduction in cell viability indicated membrane damage which was evidenced by the detected LDH leakage by 92% for the benzoyl compound while for the nitro substituted compound it was increased by 386%. Also, the least toxic benzoyl compound had no effect on the GSH levels while **1** decreased them by 42%. The MDA production, which is a marker of the lipid peroxidation, was elevated by 161% for **1** and by 124% for the substituted with a benzoyl group benzimidazole-2-thione compared to the non-treated hepatocytes.

Taking into consideration that reduction of the nitro group of **1** to a nitro radical anion (Scheme 2) might be the origin of the higher hepatotoxicity of this compound, we decided to investigate the feasibility of a nitro radical anion formation from **1** through electrochemical generation and IR measurements in DMSO solution.

The *in situ* generation of the radical anion of **1** in an electrochemical IR liquid cell was selected as a method of study based on the ability to provide detailed and useful spectral information, which can be interpreted in terms of structural characteristics [9–11]. The method allows identification of the reductive products by their characteristic IR absorptions and also observation of the changes over time. The description of the structural and spectral changes arising from the conversion was assisted by DFT computations at IEFPCM-B3LYP/6–311++G** level of theory with inclusion of DMSO as a solvent. Structure characterization by computational methods of a highly reactive and unstable intermediate, such as radical-anions, has been proven as accurate and reliable, especially when correlated with spectral characteristics or other directly observable properties to support the structural predictions [12,13].

2. Material and methods

2.1. Used materials

Methyl 3-[3-(3-methoxy-3-oxopropyl)-5-nitro-2-thioxo-2,3-dihydro-1H-benzimidazol-1-yl]propanoate (**1**) was synthesiszed

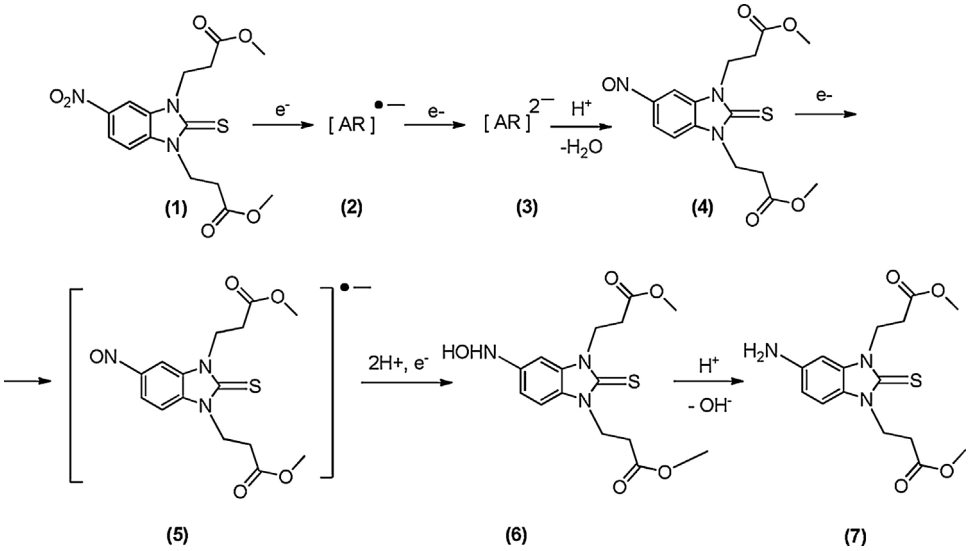

Scheme 2. Hypothetical reductive products of methyl 3-[3-(3-methoxy-3-oxopropyl)-5-nitro-2-thioxo-2,3-dihydro-1H-benzimidazol-1-yl]propanoate.

according to the procedure reported by us earlier [8] and recrystalized in methanol. Tetrabutylammonium bromide (99%) was purchased from Merck and used without futher purification. Spectral quality $CDCl_3$ and DMSO-d_6 were purchased from Sigma-Aldrich Co.

2.2. Experimental procedure

The spectra were recorded on Bruker Tensor 27 FT spectrometer at a resolution of 2 cm^{-1} and 64 scans. The spectrum in solid state was measured by directly applying the sample on a diamond crystal ATR accessory. The spectrum in $CDCl_3$ (0.1 M) solution was recorded in a 0.2 mm KBr cell.

The assignment of exact positions to the components of broad and overlapped bands was done by deconvolution and curve-fitting procedure. The initial bandwidth of all components was set to 14 cm^{-1} and the components were approximated by mixed Lorentzian/Gaussian functions. The curve-fitting was performed according to the Local Least Squares algorithm.

The electrochemical generation of the radical anion of **1** was performed in a special CaF_2 cell provided with platinum electrodes build in the polyethylene spacer (Scheme S1) [14]. The volume of the cell is 0.2 ml, path length: 0.1 mm. 4.5 V were applied to the cathode in the solution cell containing 0.1 mol l^{-1} of **1** and an equimolar amount of tetrabutylammonium bromide in DMSO-d_6. Electrochemical reduction was carried out for a period of 100 min and then the polarity of the electrodes was reversed in order to regenerate the parent compound. The process of electrochemical reduction and regeneration of a neutral compound was monitored by recording IR spectra at 10 min intervals. The IR spectra were measured at a resolution of 2 cm^{-1} and 64 scans by referencing the electrolyte salt in DMSO-d_6 as a background.

2.3. Computational details

All theoretical calculations were performed using the Gaussian 09 package of programs [15]. Geometry and vibrational frequencies of the species studied were performed by an analytical gradient technique without any symmetric constraint. All the results were obtained using the density functional theory (DFT), employing the B3LYP (Becke's three-parameter non-local exchange correlation) functional. Incorporation of a DMSO solvent was performed by the Integral Equation Formalism of Polrizable Continuum Model (IEF-PCM), proposed by Tomasi and coworkers [16,17]. The stationary points found on the potential energy hypersurfaces for each structure were characterized using the standard harmonic vibrational analysis. A standard least-squares program has been used to calculate single parameter regression indices. The absence of imaginary frequencies confirmed that the stationary points corresponded to local minima on the potential hypersurfaces. Electron density within the molecule was characterized by natural bond orbitals (NBO) analysis [18–20].

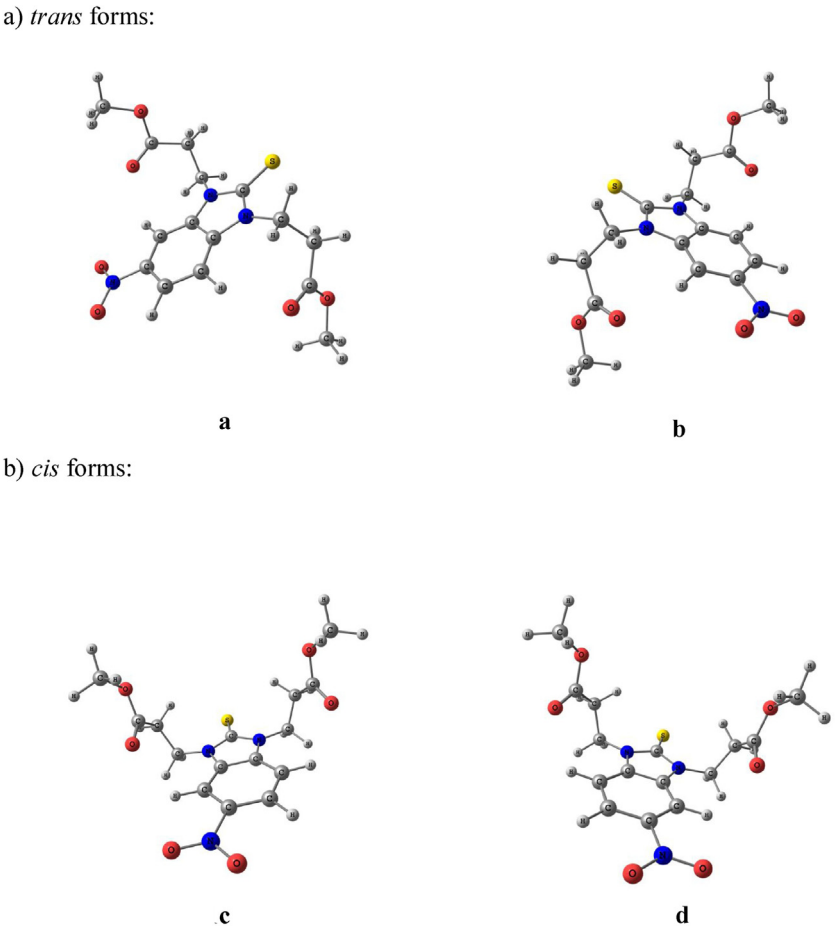

Fig. 1. Possible stereoisomers of **1**.

The assignment of the theoretical vibrational frequencies was assisted by analysis of the potential energy distributions (PEDs) using the VEDA 4 program [21].

The native theoretical IR frequencies of the neutral molecule and radical anion were scaled according to the following equation:

$$\nu^{sc} = 0.93114\nu^{native} + 84.8\ (cm^{-1}) \quad (1)$$

obtained from the linear correlation between the experimental and calculated native frequencies of the neutral compound **1**. The correlation coefficient R was 0.9894, standard deviation S. D. = 22.5 cm^{-1}; number of data points n = 19. The mean absolute deviation

$$MAD = n^{-1}\sum|(\rho\nu_i^{theor.(native)} + b) - \nu_i^{exp.}| \quad (2)$$

was used as a measure for the deviation between the theoretical and experimental values.

Adiabatic electron affinity (EA) i.e. the enthalpy of formation of the radical anion was calculated according to the following equation:

$$EA = H(\text{radical anion}) - H(\text{neutral molecule}) - H(e^-) \quad (3)$$

The enthalpies were calculated for 298 K, in DMSO solvent. Solvation enthalpy of electron, $H(e^-)$ in DMSO was determined as $H(e^-)_{solv} = H(DMSO^{\cdot-})_{solv} - H(DMSO)_{solv} - H(e^-)_{gas}$ where $H(e^-)_{gas}$ is 3.145 kJ mol^{-1} [22].

3. Results and discussion

3.1. Molecular geometry

The preferred geometry of the neutral methyl 3-[3-(3-methoxy-3-oxopropyl)-5-nitro-2-thioxo-2,3-dihydro-1H-benzimidazol-1-yl]propanoate and its radical anion was established based on optimization and energy analysis of the most probabale conformers in DMSO. Several extended and folded conformations were considered for the alkyl chains attached to N1 and N3, as well as different orientations of the two chains in respect to the flat benzimidazole-2-thione fragment.

Orientation of the two N-alkyl chains at opposite sides of the plane of the benzimidazole-2-thione fragment was denoted as a *trans* conformation, while those at the same side of the plane as a *cis* conformation, respectively. Due to the presence of the nitro

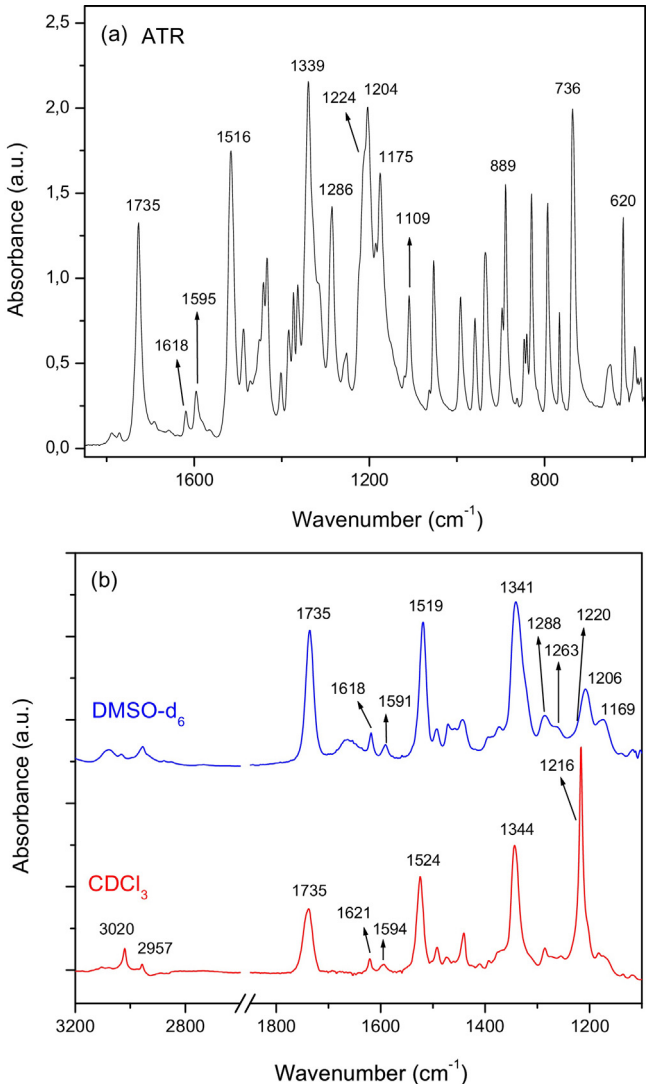

Fig. 2. Experimental IR spectra of **1**: (a) ATR spectrum in solid state; (b) absorbance IR spectrum DMSO-d_6 (in blue) and in $CDCl_3$ (in red). (For interpretation of the references to colour in this figure legend, the reader is referred to the web version of this article.)

Table 1
Theoretical IEFPCM-B3LYP/6-311++G** and experimental (solvent DMSO-d_6) IR wavenumbers ($\tilde{\nu}$ in cm^{-1}) and integrated intensities (A) of the neutral **1** in DMSO solvent.

No	Theoretical data			Experimental data[a]			
				DMSO-d_6		ATR	
	$\tilde{\nu}_{theor.}$[b]	A[c]	Approximate description[d]	$\tilde{\nu}_{exp.}$	A[e]	$\tilde{\nu}_{exp.}$	A[e]
1.	3110	24.1	ν^{Bz}(C-H)	3080[f]	vw	3070	w
2.	3097	4.5	ν^{Bz}(C-H)	-[g]	-[g]	3036	w
3.	3087	1.5	ν^{Bz}(C-H)	3020[f]	w	2996	w
4.	3036	15.8	$\nu^{as}(CH_3)$	2957[f]	w	2953	w
5.	3036	15.5	$\nu^{as}(CH_3)$				
6.	3013	2.4	$\nu^{as}(CH_2)$	-[g]		-[g]	
7.	3011	2.3	$\nu^{as}(CH_2)$	-[g]		-[g]	
8.	3006	24.7	$\nu^{as}(CH_3)$	-[g]		-[g]	
9.	3006	26.0	$\nu^{as}(CH_2)$	-[g]		2932	w
10.	2987	3.7	$\nu^{as}(CH_2)$	-[g]			
11.	2985	4.0	$\nu^{as}(CH_2)$	-[g]		-[g]	
12.	2965	18.3	$\nu^{s}(CH_2)$	-[g]		-[g]	
13.	2963	18.5	$\nu^{s}(CH_2)$	-[g]		-[g]	
14.	2933	32.3	$\nu^{s}(CH_3)$	-[g]		2872	w
15.	2933	31.4	$\nu^{s}(CH_3)$	-[g]			
16.	2921	7.9	$\nu^{s}(CH_2)$	-[g]		2850	w
17.	2921	9.6	$\nu^{s}(CH_2)$	-[g]		-[h]	
18.	1714	540.	ν(C=O)	1735	s	1727	s
19.	1713	348.7	ν(C=O)				
20.	1612	81.5	ν^{Bz}(C=C)	1618	m	1618	w
21.	1612	37.5	ν^{Bz}(C=C)	1591	w	1595	w
22.	1510	454.6	$\nu^{as}(NO_2)$	1519	vs	1516	vs
23.	1490	217.8	δ^{Bz}(CCH)	1492	m	1487	m

24.	1468	6.2	$\delta^{as}(CH_3)$					
25.	1468	37.6	$\delta^{as}(CH_3)$	}	1471	m	} 1472	m
26.	1468	26.9	$\delta^{as}(CH_3)$					
27.	1466	170.5	$\delta(CH_2)$	}	1458	m	} 1462	m
28.	1460	57.0	$\delta(CH_2)$					
29.	1459	14.4	$\delta^{as}(CH_3)$		[g]		} 1451	sh
30.	1459	17.4	$\delta^{as}(CH_3)$					
31.	1452	47.2	$\delta^{s}(CH_3)$	}	1443	w	} 1442	m
32.	1452	7.0	$\delta^{s}(CH_3)$					
33.	1437	3.7	$\delta(CH_2)$	}	1434	sh	} 1433	s
34.	1435	4.7	$\delta(CH_2)$					
35.	1423	388.6	$\delta(CCH), \nu^{Bz}(C\text{-}N)$		1394	w	1402	w
36.	1399	40.8	$\gamma(CH_2)$	}	1387	w	} 1384	m
37.	1398	90.0	$\gamma(CH_2)$					
38.	1389	35.1	$\gamma(CH_2)$	}	1373	w	} 1373	m
39.	1387	112.6	$\gamma(CH_2)$					
40.	1377	273.2	$\nu^{Bz}(C\text{-}N), \nu^{Bz}(CC)$		1365	m	1363	m
41.	1373	218.8	$\nu^{Bz}(C\text{-}N), \delta(CNC)$		[g]		[g]	
42.	1346	204.8	$\delta(NCH), \nu^{Bz}(C\text{-}N)$		[g]		[g]	
43.	1327	83.6	$\nu^{Bz}(C\text{-}N), \delta(CCH)$		[g]		[g]	
44.	1318	1547.7	$\nu^{s}(NO_2)$		1341	vs	1339	vs
45.	1282	48.2	$\delta^{Bz}(CCH)$		[g]		[g]	
46.	1268	722.7	$\gamma(CH_2)$	}	1288	w	} 1286	m
47.	1247	38.3	$\gamma(CH_2)$					sh
48.	1244	558.0	$\nu(C\text{-}O)$	}	1263	w	}	1258 w
49.	1223	18.6	$\nu(C\text{-}O)$					1252 sh
50.	1213	228.1	$\nu(C{=}S), \nu^{Bz}(CC)$		1220	sh	1224	sh
51.	1203	8.2	$\gamma(CH_3)$		[g]		1212	sh

52.	1199	176.5	ν(C-O), $\gamma(CH_3)$	1206	m	1204	s
53.	1185	78.6	ν^{Bz}(C-N), δ^{Bz}(CCH)	1184	m	1185	m
54.	1182	24.1	ν^{Bz}(CC), ν^{Bz}(C-N)	1169	m	1175	s
55.	1172	4.5	$\gamma(CH_3)$	-[g]		-[g]	
56.	1172	1.5	$\gamma(CH_3)$	-[g]		-[g]	
57.	1151	15.8	δ^{Bz}(CCH)	-[g]		-[g]	
58[i]	1110	15.5	ν(C-NO_2), ν(CC)	-[g]		1109	m
mad[h]				***10.4***			

[a]Measured after having decomposed the complex bands into components. [b]Infrared wavenumbers [cm^{-1}] scaled by Eq. (1). [c]Predicted intensities [km mol^1]. [d]Vibrational modes: ν, stretching; δ, in-plane bending; γ, out of plane banding; superscripts: s – symmetrical, s – asymetrical, Bz – benzimidazole; [e]Relative intensities: vw, very weak; w, weak; m, moderate; s, strong; vs, very strong; sh, shoulder; [f]Measured in $CDCl_3$. [g]These bands were not detected in the IR spectrum. [h]Followed by 62 lower-frequency vibrations. [i]Mean Absolute Deviation between theoretically predicted and experimentally observed IR wavenumbers.

group at 5-position of the benzimidazole-2-thione fragment, each of these forms has two enantiomers. The geometries of all constructed isomers were fully optimized and characterized using standard analytical harmonic vibrational analysis. The absence of imaginary frequencies, as well as of negative eigenvalues of the second-derivative matrix, confirmed that the stationary points correspond to the minima on the potential energy hypersurface.

According to the energy analysis, the *cis* form of **1** is more stable by 0.19 kJ mol^{-1}. The benzimidazole-2-thione fragment is flat and well conjugated with the nitro group lying in the same plane (Fig. 1). The geometry is stabilized by the intramolecular interactions between the phenyl H-atoms to the carbonyl groups and the methylene H-atoms to S. Similar interactions were identified in the recently reported crystal structures of unsubstituted and 5-benzoyl substituted methyl 3-[3-(3-methoxy-3-oxopropyl)-2-thioxo-2,3-dihydro-1H-benzimidazol-1-yl]propanoate [8].

The energy difference between the *cis* and *trans* forms of the radical anion **2** is 0.10 kJ mol^{-1}. The further theoretical description of the structure and IR spectra of anion radical **2** was carried out by using the *cis* conformation.

3.2. IR spectral characterization of neutral compound 1

In order to achieve an accurate and reliable description of the changes accompanying the electrochemical reduction of **1**, it is necessary first to investigate the IR spectra of the neutral parent compound and to assign the observed IR bands to the corresponding molecular vibrations. For this purpose, the IR spectra of **1** were measured in solid state (ATR), in $CDCl_3$ and DMSO-d_6 solution (Fig. 2). Despite its shorter region (4000–1100 cm^{-1}), the IR spectrum of **1** in DMSO-d_6 is very important, because the electrochemical reduction will be carried out in the same solvent. Therefore, the bands positions in DMSO-d_6 will be discussed in more detail. The experimental data for **1** measured in DMSO-d_6 solution in the 4000–1100 cm^{-1} region are compared to the theoretically calculated wavenumbers in Table 1. Due to broadening and overlapping of some bands, the assignment of exact positions to their components was done by deconvolution and curve-fitting procedure.

The most intense bands at 1519 and 1341 cm^{-1} in the spectrum measured in DMSO-d_6 solution correspond to the assymetric and symmetric stretching vibration of the nitro group. The stretching vibrations of the two carbonyl groups give rise to one strong band at 1735 cm^{-1}. The presence of only one band can be expalined by the larger distance between the two groups preventing the coupling of their stretching and also by the fact that the adjacent methyl and methylene groups have equal influence. According to the theoretical calculations the two carbonyl stretching freqnecies are virtually identical (Table 1). The same could be observed regarding the methyl and methylene groups of the side chains. For instance, the assymetric stretching vibrations of the two methyl groups have identical wavenumbers and only one weak band appeared at 2957 cm^{-1} in $CDCl_3$.

According to the calculations, a band of moderate intensity is expected around 1100 cm^{-1} for the stretching vibration of the C—NO_2 band. It is known from literature that ν(C—NO_2) of nitrobenzene gives rise to a band at 1108 cm^{-1} in liquid state [23] and the same vibration in 2-methyl-5-nitroimidazole is characterized by a band at 1104 cm^{-1} [24]. Based on these experimental observations and the theoretically predicted length of ν(C—NO_2) in **1**, a moderately intensive band at 1109 cm^{-1} in solid state was recognized as ν(C—NO_2). In DMSO-d_6 solution the band cannot be observed due to the self-absorptions of the CaF_2 cell.

As could be seen from the reported studies, the position of the band for the stretching vibration of the C=S group can vary in a broad range. For example, in the spectrum of 5-nitrobenzimidazole-2-thione in solid state, the band is observed at 1189 cm^{-1} while the presence of an N-substituent at position 1 causes a shift to the higher wavenumbers and it appears in the range 1210–1230 cm^{-1} [25]. A similar wavenumber range (1150–1220 cm^{-1}) can be seen also for 1-alkylimidazole-2-thiones [26]. All this implies that the frequency of ν(C=S) is very sensitive to the presence and the nature of the substituents in the benzimidazole ring. The theoretical calculations in DMSO solution predicted that the corresponding vibration is strongly mixed with those of the neighboring atomic groups and that the band is expected at 1213 cm^{-1}. In the DMSO-d_6 spectrum the band was found after deconvolution procedure (Fig. S1) at 1220 cm^{-1}, strongly overlapped with the neighboring bands at 1206 and 1263 cm^{-1} attributed to ester C—O stretchings.

The relative intensities of the IR bands of **1** in solid state, polar DMSO-d_6 and nonpolar $CDCl_3$ solution differ markedly (Fig. 2). It is known that the IR intensities not only depend on the chemical environment i.e. solvent, phase change, intermolecular interactions, etc., but the effect of a given solvent on different vibration

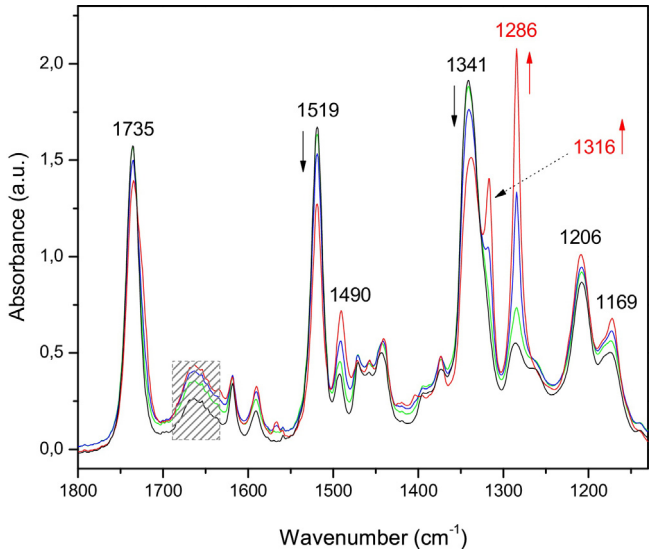

Fig. 3. Infrared spectra of **1** in DMSO-d_6 (0.1 mol l^{-1}) measured in the course of electrochemical reduction: t = 0 min (in black); t = 30 min (in green); t = 60 min (in blue); t = 100 min (in red); striped area – water absorptions due to solvent moisture;. (For interpretation of the references to colour in this figure legend, the reader is referred to the web version of this article.)

bands is different [27]. In the present case it is evidenced by the enhanced relative intensity of ν(C = S) in nonpolar $CDCl_3$ (Fig. 2b). Increased IR intensity in chloroform solution in comparison to DMSO were reported previously for cyano stretching vibration in benzonitrile [28,29].

3.3. Electro-chemical reduction of 1

The electrochemical reduction was carried out *in situ* in the IR liquid cell on a 0.1 mol l^{-1} solution of the parent compound **1** in DMSO-d_6, containing tetraethylammonium bromide as electrolyte salt. The initial solution of the parent compound was yellow as the solid product.

As a result of the applied potential, the solution in the cathode space started changing its color to green which was intensified over time. The intensity of the bands for the nitro stretching vibrations of the parent neutral compound started gradually decreasing. At the same time, new bands appeared in the IR spectrum at 1316 and 1286 cm^{-1} (Fig. 3). More prolonged electrolysis (100 min) caused a considerable increase of the new bands, while the reduction of the nitro bands of the neutral compound continued. Reversal in the polarity of the electrolysis cell resulted in reappearance of the yellow color and vanishing of the IR bands of the new product. This fact demonstrates that the observed spectral changes should be attributed to the reduction of **1** to a radical anion and not to chemical transformation to other products.

In order to confirm this assumption, the frequncies of the bands appearing in the course of the electrochemical reduction were compared with the ones theoretically calculated for the radical-anion of **1** (Table 2). The comparison of the experimental and the theoretical frequencies enables the accurate assignment of the observed bands of the molecular vibrations of the radical anion **2**. This would be considerably more difficult were it based only on the experimental data as the spectral studies on highly reactive and unstable nitro radical anions are insufficient.

The data presented in Table indicates that the conversion of the molecule into a radical anion **2** is expected to lead to a considerable drop of the wavenumber for $\nu^{as}NO_2$–from 1510 cm^{-1} in the parent neutral compounds to 1240 cm^{-1} in the radical anion. Indeed, as a result of the reduction, the appearance of a very intensive band is observed, which must be attributed to that vibration. Thus the experimentally measured drop of the wavenumber for $\nu^{as}(NO_2)$ is 233 cm^{-1} and corresponds quite well to the theoretically calculated value – 270 cm^{-1}. As assumed from the theoretical spectrum of **2**, the band responsible for the nitro group symmetrical stretching vibration shifts significantly to the lower wavenumbers (more than 241 cm^{-1}) and is not observed, since it falls in the region under 1100 cm^{-1}. The theoretically predicted drop of the wavenumber for $\nu^{s}(NO_2)$ is 221 cm^{-1}.

The conversion of the molecule into a radical anion is expected to bring about the increase of the band wavenumber for ν(C—NO_2) by 223 cm^{-1}. Based on the **2** theoretical spectrum it is expected at 1322 cm^{-1}. This indicates that the experimentally observed band at 1316 cm^{-1} corresponds to the stretching vibration of the C—NO_2 bond.

In the radical anion spectrum ν(C=O) practically do not change their frequency, while those of the benzimidazole ring preserve their frequencies, but increase their intensities (Table 2). These theoretically predicted changes also correspond quite well to the spectrum observed in the electrochemical reduction of **1**.

The scaling of the native theoretical IR wavenumbers provided a very good agreement between experimental and theoretical wavenumbers – 10.4 cm^{-1} is MAD for the neutral compound **1** and 11.2 cm^{-1} for radical anion **2**, respectively. These values lie on the bottom border of the interval 9–25 cm^{-1} determined recently for organic molecules and anions containing carbonyl- and cyanogroups [9–11]. The values of MAD are also very close to these observed for cyano stretch in a large series of radical anions of nitriles [12], but they are higher than those observed for carbonyl stretch in ketyls [13]. However, when estimating the accuracy of the predictions, it should be taken into account that description of one vibrational mode, such as cyano or carbonyl stretch, should be expected to be more accurate than the description of various vibrational modes including stretch, in-plane, and out-of-plane deformations. The theoretical level and influence of the solvent are also very important in the calculation of theoretical wavenumbers.

Table 2
Theoretical IEFPCM-B3LYP/6–311++G** and experimental (solvent DMSO-d_6) IR wavenumbers ($\tilde{\nu}$ in cm^{-1}) and integrated intensities (A in $km\,mol^{-1}$) of the anion-radical **2.**

No	Theoretical data			Experimental data[a]	
	$\tilde{\nu}_{theor.}$[b]	A[c]	Approximate description[d]	$\tilde{\nu}_{exp.}$	A[f]
1.	3105	4.4	ν^{Bz}(C-H)	-[f]	-[f]
2.	3090	2.4	ν^{Bz}(C-H)	-[f]	-[f]
3.	3071	0.8	ν^{Bz}(C-H)	-[f]	-[f]
4.	3035	19.8	$\nu^{as}(CH_3)$	-[f]	-[f]
5.	3035	19.9	$\nu^{as}(CH_3)$	-[f]	-[f]
6.	3007	4.5	$\nu^{as}(CH_2)$	-[f]	-[f]
7.	3005	28.5	$\nu^{as}(CH_2)$	-[f]	-[f]
8.	3005	28.9	$\nu^{as}(CH_3)$	-[f]	-[f]
9.	3005	3.7	$\nu^{as}(CH_2)$	-[f]	-[f]
10.	2993	5.5	$\nu^{as}(CH_2)$	-[f]	-[f]
11.	2991	5.1	$\nu^{as}(CH_2)$	-[f]	-[f]
12.	2959	26.4	$\nu^{s}(CH_2)$	-[f]	-[f]
13.	2957	21.1	$\nu^{s}(CH_2)$	-[f]	-[f]
14.	2933	28.8	$\nu^{s}(CH_3)$	-[f]	-[f]
15.	2932	35.7	$\nu^{s}(CH_3)$	-[f]	-[f]
16.	2921	9.4	$\nu^{s}(CH_2)$	-[f]	-[f]
17.	2919	10.6	$\nu^{s}(CH_2)$	-[f]	-[f]

18.	1713	341.2	ν(C=O)	1735	s
19.	1713	325.4	ν(C=O)		
20.	1603	114.0	ν^{Bz}(C=C)	1618	w
21.	1577	7.0	ν^{Bz}(C=C)	1591	w
22.	1479	9.0	δ^{Bz}(CCH)	1490	m
23.	1469	9.2	$\delta^{as}(CH_3)$	1471	m
24.	1468	113.4	$\delta^{as}(CH_3)$		
25.	1466	10.3	$\delta(CH_2)$	-[f]	-[f]
26.	1462	10.2	$\delta(CH_2)$	-[f]	-[f]
27.	1460	39.1	$\delta(CH_2)$	-[f]	-[f]
28.	1460	64.7	$\delta^{as}(CH_3)$	1457	m
29.	1459	29.0	$\delta^{as}(CH_3)$		
30.	1452	15.7	$\delta^{s}(CH_3)$	-[f]	-[f]
31.	1452	7.4	$\delta^{s}(CH_3)$	-[f]	-[f]
32.	1443	24.3	$\delta(CH_2)$	1440	m
33.	1440	8.7	$\delta(CH_2)$		
34.	1416	231.2	ν^{Bz}(C-N), $\gamma(CH_2)$	-[f]	-[f]
35.	1400	8.6	ν^{Bz}(C-N), $\gamma(CH_2)$	-[f]	-[f]
36.	1394	48.2	$\gamma(CH_2)$	-[f]	-[f]
37.	1383	120.5	ν^{Bz}(C-N), $\gamma(CH_2)$	1374	w
38.	1377	101.0	ν^{Bz}(C=C), ν^{Bz}(C-N), $\gamma(CH_2)$	-[f]	-[f]

39.	1374	269.9	ν^{Bz}(C-N), ν(C-NO_2), $\gamma(CH_2)$	-[f]	-[f]
40.	1366	288.3	$\gamma(CH_2)$	-[f]	-[f]
41.	1359	127.9	$\gamma(CH_2)$	-[f]	-[f]
42.	1336	175.6	ν^{Bz}(C-N), δ(CCH)	-[f]	-[f]
43.	1322	251.7	ν(C-NO_2), ν^{Bz}(C-N), $\gamma(CH_2)$	1316	vs
44.	1270	152.0	ν(C-O), $\gamma(CH_2)$	-[f]	-[f]
45.	1262	134.5	ν(C-O), $\gamma(CH_2)$	-[f]	-[f]
46.	1253	322.7	δ^{Bz}(CCH)	-[f]	-[f]
47.	1248	95.0	$\gamma(CH_2)$	-[f]	-[f]
48.	1240	500.0	$\nu^{as}(NO_2)$	1286	vs
49.	1217	288.7	ν(C-O), $\gamma(CH_2)$	1206	s
50.	1209	25.0	$\gamma(CH_3)$	-[f]	-[f]
51.	1203	40.0	$\gamma(CH_3)$	-[f]	-[f]
52.	1193	255.4	ν(C=S), $\gamma(CH_3)$	-[f]	-[f]
53.	1182	210.5	ν^{Bz}(C-N), δ^{Bz}(CCH)	-[f]	-[f]
54.	1173	2.1	$\gamma(CH_3)$	-[f]	-[f]
55.	1172	1.8	ν^{Bz}(CC)	-[f]	-[f]
56.	1172	32.6	$\gamma(CH_3)$	-[f]	-[f]
57.	1138	28.6	δ(CCH)	-[f]	-[f]
58[g]	1097	52.5	$\nu^{s}(NO_2)$, ν^{Bz}(CC)	-[f]	-[f]
mad[h]				***11.2***	

[a]Measured after having decomposed the complex bands into components. [b]Infrared wavenumbers [cm^{-1}] scaled by Eq. (1). [c]Predicted intensities [km mol^{-1}]. [d]Vibrational modes: ν, stretching; δ, in-plane bending; γ, out of plane banding; superscripts: s – symmetrical. s – asymetrical, Bz – benzimidazole; [e]Relative intensities: vw, very weak; w, weak; m, moderate; s, strong; vs, very strong. [f]These bands were not detected in the IR spectrum. [g]Followed by 62 lower-frequency vibrations. [h]Mean Absolute Deviation between theoretically predicted and experimentally observed IR wavenumbers.

The inability to detect some of the bands of radical anion **2** which overlap with the bands of the parent neutral compound **1** makes it difficult to judge on the achieved accuracy of predicted intensities. Many authors have questioned the ability of quantum-chemical methods to predict IR intensities quantitatively and pointed out that high computational levels are required to achieve satisfactory agreement [27,30–34]. Calculation and application of scale factors to the predicted IR integrated intensities is also hindered by deficiency of stable trends toward under- or overestimation of the experimental intensities by means of computations [27].

Reappearance of the parent bands upon reversal of the electrodes polarity and the agreement between experiment and theory are evidence that **2** is obtained, and there is no observable amount of other species resulting from recombination of **2** or other chemical conversions.

3.4. Structure and stability of radical anion 2

The hepatotoxicity of nitro aromatic drugs is governed by several factors – the extent of nitro reduction, the nature of other aromatic ring substituents, the lipophilicity and the routes of metabolitic conversion to other active or inactive metabolites [5]. In this relation it is useful to study the structural characterisctics of nitroaromatic compounds which exhibited hepatotoxicity and to try to connect their chemical structure to the propensity to generate nitro radical anions. Such correlations can improve the understanding of the mechanisms underlying the hepatotoxicity of a particular group of compounds and help to suggest a strategy how to reduce the toxicity by structural modifications. For these reasons, interpretation of the observed spectral changes in light of concomitant structural changes represents an important part of the present study.

The increase in the frequency of the C—NO_2 bond is evidence for its shortening and increase of its bond order. The opposite is observed for the N—O bonds – they lengthen and their bond order decreases significantly. These conclusions are confirmed also by the theoretically calculated bond lengths in the radical anion **2** (Table A1, Appendix). In general, it can be concluded that the structural changes are most significant in the planar 5-nitrobenzimidazole-2-thione fragment. The structural variations in the C—NO_2 moiety are accompanied by strong lengthening of the C—C bonds adjacent to the nitro group, lengthening of the C=S bond, and rearrangement of the C—N bond lengths in an alternating manner (Table A1, Appendix). Hence **2** is characterized by a wider and more strongly conjugated electron system than the neutral parent compound **1** and the formation of a quinoid-like structure. The tendency of the spectral and structural changes is similar to those observed in nitrobenzene [35]. Studies have shown that the coplanar orientation of the nitro group towards the aromatic system is related to higher toxicity than when it is positioned perpendicularly [36] which could be explained by the inability of the nitroreductase to react with the molecule in the perpendicular orientation [37]. From the theoretical calculations it can be concluded that the neutral compound **1** and the radical anion **2** exhibit coplanar structure and this most likely contributes to the observed toxicity.

An important structural characteristic of the radical anion is the degree of delocalization of the odd electron over the conjugated system. It is known from previous research that when aromatic compounds are converted into radical anions the higher the degree of localization of the unpaired electron (spin density) on a definite functional group, the higher its frequency drop of the stretching vibration [13]. Having in mind the significant nitro group vibration frequency drop observed in the reduction of **1** it can be assumed that the unpaired electron is localized, to a considerable degree, on the nitro group. For the better clarification of this important characteristic, a theoretical analysis of the spin density of **2** was carried out. The results are presented in Scheme 3.

The NBO spin population analysis showed that 0.707 of the odd electron is localized over the nitro group of **2**, while 0.293 is spread over the benzimidazole fragment (Scheme 3a). The localization of the odd electron depends on the nature of the aryl system bearing the nitro substituent and also on the presence of other substituents. In order to estimate the importance of the constituting molecular fragments in **2** (benzimidazole ring, N-alkyl chains, thione function), the analysis on the spin density distribution was extended by including 5-nitrobenzimidazole-2-thione and 5-nitrobenzimidazole (Scheme 3b and c). Obviously the presence of N-alkyl chains slightly enhances the localization of the

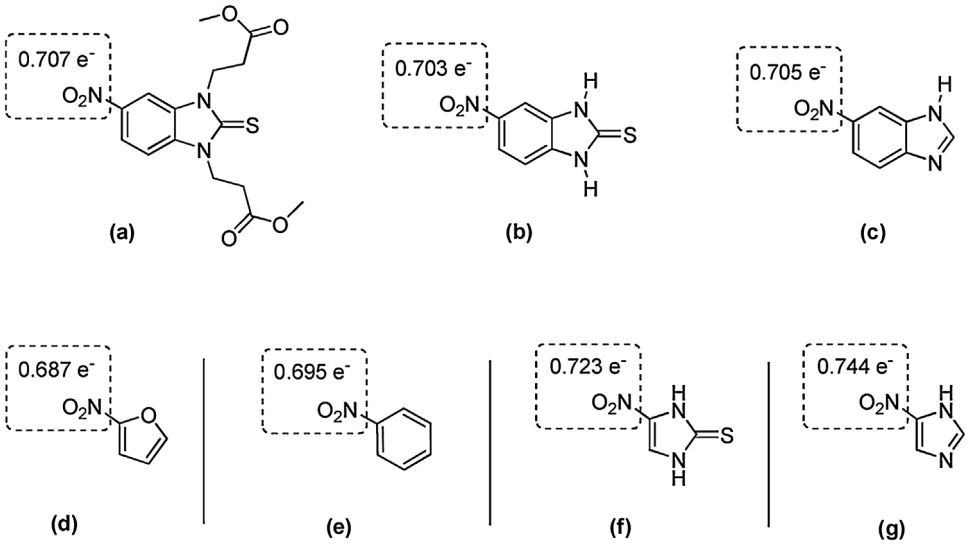

Scheme 3. Spin density distribution over fragments in the radical anions of **2** (a); 5-nitrobenzimidazole-2-thione (b); 5-nitrobenzimidazole (c); 2-nitrofuran (d); nitrobenzene (e); 5-nitro-imidazole-2-thione (f); and 5-nitroimidazole (g).

odd electron over the nitro group as evidenced by the spin density distribution in **2** and 5-nitrobenzimidazole-2-thione. On the other hand, considering the higher value for the nitro group in the 5-nitrobenzimidazole, it can be concluded that the thione function contributes to the more effective delocalization of the odd electron over the conjugated system, and therefore stabilizes the radical anion.

Scheme 3 illustrates also the variation of spin density distribution for some nitroaryl ring systems encountered in anticancer, antibiotic and anti-parasitic drugs. It can be seen that the nitro groups attached to furan and benzene rings bear lower spin density, while the nitro group in the imidazole ring (including imidazole-2-thione) shows a much greater value. The stabilizing effect of the thione function is demonstrated furthermore by the reduction of the spin density over the nitrogroup in 5-nitro-imidazole-2-thione in comparison to 5-nitroimidazole. The stability of the radical anion of **2** should be considered as closer to that of nitrobenzene systems than to that of nitroimidazoles. The odd electron delocalization in nitrobenzene is well known from earlier EPR studies (the nitro group retains about 0.65–0.70 of the unit spin density) [38] and having in mind the good agreement with calculation results [39], the computational estimation of the spin distribution should be regarded as a reliable tool to represent the odd electron delocalization in nitrobenzimidazoles radical anions in real systems.

The hepatotoxicity of nitroaryl compounds mediated by reactive metabolites is generally dependent on the nitroreduction rate [1–5]. Therefore, characterizing the relative ease of the reduction of **1** and comparing it to other known nitroaryl drugs would provide important estimation of the likelihood to produce hepatotoxicity. For this purpose various molecular properties have been used as a measure [40]: energy of the lowest unoccupied molecular orbital (E_{LUMO}) for the neutral compound, energy difference between the lowest unoccupied and the highest occupied molecular orbital ($\Delta E_{L\text{-}H}$), and electron affinity (EA). EA i.e. the enthalpy of formation of the radical anion might be calculated either by the optimized geometry of the neutral molecule and the radical anion (adiabatic EA) or by using the optimized geometry for the neutral molecule to calculate the energies of both the neutral and anion species (vertical EA). E_{LUMO} for a neutral gas-phase compound can provide an approximation to the vertical EA.

Molecular properties (E_{LUMO}, $\Delta E_{L\text{-}H}$, adiabatic EA and energy difference between the radical anion and the molecule $\Delta E_{M\rightarrow RA}$) involved in one-electron reduction of **1** to radical anion **2** were computed and compared to the respective values of other nitroaryl compounds and drugs. The calculated parameters were correlated with available experimental data for reduction potentials determined by pulse-radiolysis [2,41,42]. The data are gathered in Table 3. According to the calculation data the introduction of a thione function in the benzimidazole ring lowers the EA which indicates that nitrobenzimidazole-2-thiones have smaller propensity to generate nitro radical anions than 5-nitrobenzimidazoles. The presence of N-alkyl chains in the benzimidazole ring is also favorable, but the effect is smaller. The variation in $\Delta E_{M\rightarrow RA}$ among the studied nitrobenzimidazoles shows the same trend as EA.

The EA, E_{LUMO} and $\Delta E_{M\rightarrow RA}$ values of **1** are very close to those of nitrobenzene. The introduction of a second electron acceptor group in the aromatic ring facilitates the nitro reduction. Accordingly, it can be seen from Table 3 that p-nitrobenzaldehyde and p-nitroacetophenone are characterized by higher EA and lower E_{LUMO}. The same relationship was established based on experimental data from pulse-radiolysis [2,41,42]. Nimesulide, which does not contain electron acceptor substituents, shows molecular characteristics similar to nitrobenzene.

On the other hand, based on the higher EA, nitrofuran would undergo a much easier nitro reduction than nitrobenzene. The electronic interaction of the nitro group in nitrofurantoin with the additional fragments present in its structure leads to significantly higher nitro reduction rates and hepatotoxicity.

Taking into account the molecular properties characterizing **1,** it could be expected that the propensity of **1** to generate a radical anion in biological systems is comparable to that of nitrobenzene and nimesulide and much lower than those of nitrofurantoin.

4. Conclusions

The feasibility of methyl 3-[3-(3-methoxy-3-oxopropyl)-5-nitro-2-thioxo-2,3-dihydro-1H-benzimidazol-1-yl]propanoate to generate a radical anion was successfully demonstrated by electrochemical reduction combined with IR measurements. The

Table 3
Molecular properties characterizing one-electron reduction of the nitro group in **1** and several nitroaryl compounds and drugs.

Species	E_{LUMO} (eV)	ΔE_{L-H} (eV)	$\Delta E_{M\rightarrow RA}$[a] (kJ)	EA (kJ mol^{-1})	RP[b] (V)
1	−3.09	3.20	340.3	−256.1	n.a.
Nitrobenzimidazole-2-thiones					
5-Nitrobenzimidazole-2-thione	−3.15	3.07	341.3	−257.3	n.a.
5-Nitrobenzimidazole	−3.04	4.10	346.5	−261.1	n.a.
Nitrofurans					
Nitrofurantoin	−3.39	3.36	367.6	−283.2	−0.26
2-Nitrofuran	−3.22	4.34	348.8	−264.5	−0.33
Nitrobenzenes					
Nimesulide	−3.08	3.77	346.2	−262.3	−0.52[d]
p-Nitrobenzaldehyde	−3.51	4.33	369.8	−286.3	−0.32[c]
p-Nitroacetophenone	−3.41	4.22	378.3	−295.1	−0.35[c]
Nitrobenzene	−3.10	4.66	341.5	−257.3	−0.49

[a] $\Delta E_{M\rightarrow RA} = E_M - E_{RA}$.
[b] Reduction potential, determined by pulse-radiolysis [2]: higher RP (more positive) denotes more electron-affinic nitro compound.
[c] Data from [32].
[d] Data from [33].

higher hepatotoxicity demonstrated by this compound compared to other 1,3-disubstituted-1H-benzo[d]imidazole-2(3H)-thiones, could be due to bioreduction of the nitro group and emerging nitro radical anion followed by other reactive intermediates. The IR data showed that the conversion into radical anion causes:

- Strong decrease of the wavenumber for $\nu^{as}NO_2$: $\Delta\tilde{\nu} = 270\,cm^{-1}$ (theor.); $233\,cm^{-1}$ (exp.);
- Strong decrease of the wavenumber for $\nu^{s}NO_2$: $\Delta\tilde{\nu} = 221\,cm^{-1}$ (theor.); more than $241\,cm^{-1}$ (exp.);
- Strong increase of the wavenumber for $\nu(C—NO_2)$: $\Delta\tilde{\nu} = 223\,cm^{-1}$ (theor.); more than $216\,cm^{-1}$ (exp.).

The theoretical method used gives a good description of the strong spectral changes caused by the conversion. Based on the observed IR frequency shifts and theoretical calculations it was possible to draw conclusions on several molecular characteristics related to the conversion. In summery, the neutral compound **1** and the radical anion **2** exhibit coplanar orientation of the nitro group towards the aromatic system which most likely contributes to the observed toxicity and extended electronic conjugation; the major spin density (0.707 of the odd electron) is localized over the nitro group in the radical anion; the radical anion shows extended electronic conjugation compared to the neutral compound; and the presence of thione function and N-alkyl chains in the benzimidazole ring contributes favorably to reduce the propensity for nitro radical anions generation. Finally, by analyzing the calculated energies of the lowest unoccupied molecular orbital (E_{LUMO}), energy differences between the lowest unoccupied and the highest occupied molecular orbital ($\Delta E_{L\text{-}H}$), adiabatic electron affinities (EA), and energy difference between the radical anion and the molecule ($\Delta E_{M\rightarrow RA}$) for **1** and other nitroaryl compounds, it was found that the ease of nitro reduction of methyl 3-[3-(3-methoxy-3-oxopropyl)-5-nitro-2-thioxo-2,3-dihydro-1H-benzimidazol-1-yl]propanoate in biological systems should be comparable to that of nitrobenzene and nimesulide and much lower than those of nitrofurantoin.

Acknowledgement

The financial support of this work by the National Science Fund of Bulgaria (Contracts RNF01/0110), Science Fund is gratefully acknowledged.

References

[1] S.N.J. Moreno, R.P. Mason, R. Docampo, Distinct reduction of nitrofurans and metronidazole to free radical metabolites by Tritrichomonas foetus hydrogenosomal and cytosolic enzymes, J. Biol. Chem. 259 (1984) 6298–6305.
[2] P. Wardman, Some reactions and properties of nitro radical-anions important in biology and medicine, Environ. Health Perspect. 64 (1985) 309–320.
[3] D.N.R. Rao, R.P. Mason, Generation of Nitro Radical Anions of Some 5-Nitrofurans, 2- and 5-Nitroimidazoles by Norepinephrine Dopamine, and Serotonin. A Possible Mechanism for Neurotoxicity caused by Nitroheterocyclic DrugsGeneration of nitro radical anions of some 5-Nitrofurans, 2- and 5-Nitroimidazoles by norepinephrine dopamine, and serotonin. a possible mechanism for neurotoxicity caused by nitroheterocyclic drugs, J. Biol. Chem. 262 (1987) 11731–11736.
[4] D. Fau, A. Berson, D. Eugene, B. Fromenty, C. Fisch, D. Pessayre, Mechanism for the hepatotoxicity of the antiandrogen, nilutamide. Evidence suggesting that redox cycling of this nitroaromatic drug leads to oxidative stress in isolated hepatocytes, J. Pharmacol. Exp. Ther. 263 (1992) 69–77.
[5] U.A. Boelsterli, H.K. Ho, S. Zhou, K.Y. Leow, Bioactivation and hepatotoxicity of nitroaromatic drugs, Curr. Drug Metab. 7 (2006) 715–727.
[6] D. Fau, D. Eugene, A. Berson, P. Letteron, B. Fromenty, C. Fisch, D. Pessayre, Toxicity of the antiandrogen flutamide in isolated rat hepatocytes, J. Pharmacol. Exp. Ther. 269 (1994) 954–962.
[7] J.C. Paterna, F. Boess, A. Stäubli, U.A. Boelsterli, Antioxidant and cytoprotective properties of D-tagatose in cultured murine hepatocytes, Toxicol. Appl. Pharmacol. 148 (1998) 117–125.
[8] N. Anastassova, A. Ts. Mavrova, D. Yancheva, M. Kondeva-Burdina, V. Tzankova, S. Stoyanov, B. Shivachev, R. Nikolova, Hepatotoxicity and antioxidant activity of some new N, N-'disubstituted benzimidazole-2-thiones, radical scavenging mechanism and structure-activity relationship, Arab. J. Chem. (2017), doi: http://dx.doi.org/10.1016/j.arabjc.2016.12.003.
[9] Y.I. Binev, M.K. Georgieva, S.I. Novkova, The conversion of phenylpropanedinitrile (phenylmalononitrile) into the carbanion followed by IR spectra, ab initio and DFT force field calculations, Spectrochim. Acta A 59 (2003) 3041–3052.
[10] A.D. Popova, M.K. Georgieva, O.I. Petrov, K.V. Petrova, E.A. Velcheva, IR spectral and structural studies of 4-aminobenzenesulfonamide (sulfanilamide)-d_0, $-d_4$, and $-^{15}N$, as well as their azanions: combined DFT B3LYP/experimental approach, Int. J. Quant. Chem. 107 (2007) 1752–1764.
[11] E.A. Velcheva, B.A. Stamboliyska, IR spectral and structural changes caused by the conversion of 3-methoxy-4-hydroxybenzaldehyde (vanillin) into the oxyanion, Spectrochim. Acta A 60 (2004) 2013–2019.
[12] S. Stoyanov, Scaling of computed cyano-stretching frequencies and ir intensities of nitriles their anions, and radicals, J. Phys. Chem. 114 (2010) 5149–5161.
[13] S.S. Stoyanov, D.Y. Yancheva, B.A. Stamboliyska, DFT study on IR spectral and structural changes caused by the conversion of substituted benzophenones into ketyl radicals, Comp. Theor. Chem. 1046 (2014) 57–63.
[14] I. Juchnovski, I. Binev, Frequencies of the cyano group in the IR-spectra of free, electrochemically generated anion-radicals of some aromatic nitriles, C. R. Acad. Bulg. Sci. 24 (1971) 483–486.
[15] M.J. Frisch, G.W. Trucks, H.B. Schlegel, G.E. Scuseria, M.A. Robb, J.R. Cheeseman, G. Scalmani, V. Barone, B. Mennucci, G.A. Petersson, H. Nakatsuji, M. Caricato, X. Li, H.P. Hratchian, A.F. Izmaylov, J. Bloino, G. Zheng, J. Sonnenberg, M. Hada, M. Ehara, K. Toyota, R. Fukuda, J. Hasegawa, M. Ishida, T. Nakajima, Y. Honda, O. Kitao, H. Nakai, T. Vreven, D.A. Montgomery, J.E. Peralta, F. Ogliaro, M. Bearpark, J.J. Heyd, E. Brothers, K.N. Kudin, V.N. Staroverov, R. Kobayashi, J. Normand, K. Raghavachari, A. Rendell, J.C. Burant, S. Iyengar, J. Tomasi, M. Cossi, N. Rega, J.M. Millam, M. Klene, J. Knox, J.B. Cross, V. Bakken, C. Adamo, J. Jaramillo, R. Gomperts, R. Stratmann, O. Yazyev, A.J. Austin, R. Cammi, C. Pomelli, J.W. Ochterski, R.L. Martin, K. Morokuma, V.G. Zakrzewski, G.A. Voth, P. Salvador, J.J. Dannenberg, S. Dapprich, A. Daniels, O. Farkas, J.B. Foresman, J.V. Ortiz, J. Cioslowski, D.J. Fox, Gaussian 09, Revision A1, Gaussian Inc., Wallingford, CT, 2009.
[16] J. Tomasi, M. Perisco, Molecular interactions in solution: an overview of methods based on continuous distributions of the solvent, Chem. Rev. 94 (1994) 2027–2094.
[17] J. Tomasi, B. Mennucci, E.J. Cances, The IEF version of the PCM solvation method: an overview of a new method addressed to study molecular solutes at the QM ab initio level, J. Mol. Struct. (Theochem.) 464 (1999) 211–226.
[18] A.E. Reed, L.A. Curtiss, F. Weinhold, Intermolecular interactions from a natural bond orbital, donor-acceptor viewpoint, Chem. Rev. 88 (1988) 899–926.
[19] J.E. Carpenter, F. Weinhold, Analysis of the geometry of the hydroxymethyl radical by the different hybrids for different spins natural bond orbital procedure, J. Mol. Struct. (Theochem.) 46 (1988) 41–62.
[20] F. Weinhold, J.E. Carpenter, The Structure of Small Molecules and Ions, in: R. Naaman, Z. Vager (Eds.), Plenum Press, New York, 1988, pp. 227–236.
[21] M.H. Jamróz, Vibrational energy distribution analysis (VEDA): scopes and limitations, Spectrochim. Acta A 114 (2013) 220–230.
[22] E. Klein, V. Lukes, M. Ilcin, DFT/B3LYP study of tocopherols and chromans antioxidant action energetics, Chem. Phys. 336 (2007) 51–57.
[23] J. Clarkson, W.E. Smith, A DFT analysis of the vibrational spectra of nitrobenzene, J. Mol. Struct. 655 (2003) 413–422.
[24] V. Arjunan, P. Ravindran, R. Santhanam, A. Raj, S. Mohan, A comparative study on vibrational conformational and electronic structure of 1,2-dimethyl-5-nitroimidazole and 2-methyl-5-nitroimidazole, Spectrochim. Acta A 97 (2012) 176–188.
[25] D. Harrison, J.T. Ralph, The infrared spectra of some benzimidazoline-2-thiones and benzimidazol-2-yl sulphides, J. Chem. Soc. B (1967) 14–15.
[26] B.V. Trzhtsinskaya, N.D. Abramova, Imidazole-2-thiones: synthesis properties structure, Sulfur Rep. 10 (1991) 389–421.
[27] B.S. Galabov, T. Dudev, Vibrational Intensities, in: J.R. Durig (Ed.), Elsevier Science, Amsterdam, 1996.
[28] O. Exner, K. Bosek, Substituent effects in infrared spectroscopy. III. Frequencies and intensities of the CN band in meta- and para-substituted benzonitriles, Collect. Czechoslov. Chem. Commun. 38 (1973) 50–61.
[29] I.G. Binev, R.B. Kuzmanova, J. Kaneti, I.N. Juchnovski, Determination of constants of anionic substituents based on nitrile infrared frequencies and intensities, J. Chem. Soc. Perkin Trans. 2 (1982) 1533–1536.
[30] M.D. Halls, H.B. Schlegel, Comparison of the performance of local gradient-corrected, and hybrid density functional models in predicting infrared intensities, J. Chem. Phys. 109 (1998) 10587–10593.
[31] P. Pulay, G. Fogarasi, G. Pongor, J. Boggs, A. Vargha, Combination of theoretical ab initio and experimental information to obtain reliable harmonic force constants. Scaled quantum mechanical (QM) force fields for glyoxal acrolein, butadiene, formaldehyde, and ethylene, J. Am. Chem. Soc. 105 (1983) 7037–7047.
[32] M. Alcolea Palafox, Recent Research and Development in Physical Chemistry, Transworld Research Network, Trivandrum, 1998, pp. 213.
[33] L. Gribov, E. Alekseev, Calculations of the IR intensities of absorption bands by the Hartree–Fock (ab initio) and density-functional methods, J. Appl. Spectrosc. 70 (2003) 327–330.

[34] B. Galabov, Y. Yamaguchi, R.B. Remington, H.F. Schaefer, High level ab initio quantum mechanical predictions of infrared intensities, J. Phys. Chem. A 106 (2002) 819–832.
[35] R. Ma, D. Yuan, M. Chen, M. Zhou, Infrared spectrum of nitrobenzene anion in solid argon, J. Phys. Chem. A 113 (2009) 1250–1254.
[36] V. Purohit, A.K. Basu, Mutagenicity of nitroaromatic compounds, Chem. Res. Toxicol. 13 (2000) 673–692.
[37] A.S. Kalgutkar, I. Gardner, R.S. Obach, C.L. Shaffer, E. Callegari, K.R. Henne, A.E. Mutlib, D.K. Dalvie, J.S. Lee, Y. Nakai, J.P. O'Donnell, J. Boer, S.P. Harriman, A comprehensive listing of bioactivation pathways of organic functional groups, Curr. Drug Metab. 6 (2005) 161–225.
[38] E.W. Stone, A.H. Maki, Hindered internal rotation and ESR spectroscopy, J. Chem. Phys. 37 (1962) 1326–1332.
[39] D.Y. Yancheva, Characterization of the structure, electronic conjugation and vibrational spectra of the radical anions of p- and m-dinitrobenzene: a quantum chemical study, Bulg. Chem. Commun. 45 (2013) 24–31.
[40] K.L. Phillips, S.I. Sandler, P.C. Chiu, A method to calculate the one-electron reduction potentials for nitroaromatic compounds based on gas-phase quantum mechanics, J. Comp. Chem. 32 (2011) 226–239.
[41] J. Sarlauskas, E. Dickancaite, A. Nemeikaite, Z. Anusevicius, H. Nivinskas, J. Segura-Aguilar, N. Cenas, Nitrobenzimidazoles as substrates for DT-diaphorase and redox cycling compounds: their enzymatic reactions and cytotoxicity, Arch. Biochem. Biophys. 346 (1997) 219–229.
[42] H.S. Mahal, M.C. Rath, T. Mukherjee, Pulse-radiolysis studies of nimesulide in aqueous solution: effect of microheterogeneous media, Res. Chem. Intermed. 29 (2003) 503–522.